

Morphological and Molecular Characterization of *Antonospora scoticae* n. gen., n. sp. (*Protozoa, Microsporidia*) a Parasite of the Communal Bee, *Andrena scotica* Perkins, 1916 (*Hymenoptera, Andrenidae*)

Ingemar Fries^{1*}, Robert J. Paxton², Jan Tengö³, Susan B. Slemenda⁴,
Alexandre J. da Silva⁴ and Norman J. Pieniazek⁴

¹Department of Entomology, Swedish University of Agricultural Sciences, Box 7044, S - 750 07 Uppsala, Sweden;
Phone +46 18 672073; Fax +46 18 672890; e-mail: ingemar.fries@entom.slu.se

²Zoologisches Institut der Universität Tübingen, Auf der Morgenstelle 28, D - 72076 Tübingen, Germany

³Ecological Research Station of Uppsala University, Ölands Skogsby 6280, S - 386 93 Färjestaden, Sweden;

⁴Division of Parasitic Diseases, National Center for Infectious Diseases, Centers for Disease Control and Prevention, Public Health Service, U. S. Department of Health and Human Services, Atlanta, Georgia, USA

Summary

The new microsporidium *Antonospora scoticae* n. gen., n. sp., a parasite of the communal bee *Andrena scotica*, is described based on light microscopy, ultrastructural characteristics and the nucleotide sequence of the small subunit ribosomal RNA coding region. The parasite is apansporoblastic and develops in close contact with the host cytoplasm. All developmental stages are diplokaryotic. Cytoplasmic fission was not observed, but the sporogony is believed to be disporoblastic. Live spores are ovocylindrical, straight to slightly curved, and measure 6.8 × 2.7 µm whereas spores fixed and stained for TEM measure 5.0 × 1.8 µm. The exospore is four-layered, with an internal single layer followed by a thicker, more electron dense layer, then another single layer followed by a thin external double layer. The polar filament is isofilar and arranged in 15–22 coils in the posterior and mid-part of the spore. The polaroplast has tightly packed lamellae that become less densely packed in the posterior region.

The coding region of the small subunit ribosomal RNA is 1371 base pairs long. Its GC content (62%) is significantly higher than previously reported for this group of organisms. The systematic position of the described microsporidium was found to be ambiguous and is discussed in the context of inconsistencies between the molecular and morphological taxonomy of microsporidia. A new genus is proposed for *A. scoticae* without defining superior taxa be-

cause the current developmental and morphological evidence is limited and partly contradictory to the molecular data. Current taxonomies of microsporidia are based on characters that are most likely polyphyletic in nature. Traditional systems of microsporidian taxonomy may need to be extensively revised, as molecular data become available.

Keywords: *Antonospora scoticae* n. gen and n. sp., *Andrena scotica*, Ultrastructure, Molecular phylogeny, Taxonomy

Introduction

Insects are well-known for being hosts of numerous microsporidia [18, 31]. Yet, in spite of the abundance of Hymenoptera, comparatively few microsporidian infections are described from hymenopteran hosts. The whole group of Apoidea (bees), over 20,000 described species [23], has only three reported species with associated microsporidia, *Nosema apis* in *Apis mellifera* [38], *Nosema ceranae* in *Apis cerana* [11] and *Nosema bombi* in *Bombus spp.* [8]. Detailed morphological descriptions for *N. apis* [10, 12], *N. ceranae* [11] and *N. bombi* [21] and molecular data for the taxonomically useful small subunit ribosomal RNA coding region (SSU-rRNA; GenBank database accession numbers U26534, U26533 and U26158 respectively) are available for all three microsporidia. For the former two

*corresponding author

species, complete SSU-rRNA sequences are known, while for *N. bombi* only a 200 bp partial sequence has been reported.

This paper reports on a new microsporidian infection in a Swedish population of the communal, fossorial and univoltine bee *Andrena scotica* Perkins, 1916 (= *Andrena jacobi* Perkins, 1921) and a new genus is created for it. The ultrastructure of the mature spore is briefly described. The complete SSU-rRNA coding region sequence for the parasite is presented, and the relation of this species to some other species of microsporidia is discussed based on the morphological and SSU-rRNA sequence data.

Current systems for classification of microsporidia are based on their morphological and developmental features [5] or on their chromosomal cycle [31]. There has been incoherent use of morphological features to generate microsporidian taxonomies [18], and inconsistencies abound between the morphologically based taxonomies of current classification systems and those generated by molecular sequence data [1, 2, 11, 25]. Here we present further evidence that supports the need for a revision of the taxonomy of microsporidia that includes both molecular and morphological information.

Materials and Methods

Emerging female imagines of the host *A. scotica* were collected in 1995 from Törnbottens Stugby on the Baltic island of Öland, southeast Sweden. The animals were dissected in insect saline and intestines, ovaries, Dufour's glands and adipose tissue. Samples were investigated in fresh squash preparations using a light microscope under phase contrast for detecting the presence of spores.

After light air-drying, permanent squash preparations were fixed in Bouin-Duboscq-Brasil solution for 4 h and stained using Heidenhein's haematoxylin or Giemsa solution. Semithin sections 1(–2 µm) of material embedded for transmission electron microscopy (TEM) were mounted for light microscopy after contrast coloring with toluidine blue. All permanent preparations were mounted in D.P.X. (BDH Chemicals Ltd., England).

Ovaries, Dufour's glands and adipose tissue to be embedded for TEM were fixed using 2.5% glutaraldehyde (v/v) in 0.2 M sodium cacodylate buffer, pH 7.4, for 12–48 h and kept refrigerated (+7 to 8 °C) during pre-fixation. The specimens were post-fixed for 2 h. in 2% OsO₄ (w/v) in 0.1 M S-colloidine buffer after washing in Na-cacodylate buffer. The tissue pieces were dehydrated in a series of ethanol solutions of ascending concentration, followed by fixation/washing/soaking in a propylene oxide solution. After dehydration, the tissue pieces were embedded in Epoxy resin (Agar 100) by routine procedures for TEM.

Ultrathin sections were mounted on copper grids, stained with uranyl acetate followed by lead citrate and examined in a Philips 201 or Philips 420 TEM at 60–80 kV. Measurements on TEM fixed material were made from photographs of the

preparations, and measurements of fresh spores from squash preparations with an eyepiece micrometer at × 1000.

DNA isolation, PCR amplification, cloning, sequencing of the SSU-rRNA coding region, and phylogenetic analysis

DNA was extracted from *A. scoticae* spores using the glass-beads/Laureth method [29]. The region coding for the entire SSU-rRNA was amplified by PCR using primers MICROF (5'-CACCAAGGTTGATTCTGCCTGA-3') and 1492N-5 (5'-TCAACCGTAGCCTTGTTACGACTT-3'). An amplification product of about 1,400 bp was cloned using the pCR-Script Cloning kit (Stratagene, La Jolla, Calif.). To compensate for random and Taq polymerase errors [35], both strands of three independent clones were sequenced manually using custom sequencing primers and a consensus sequence of 1371 bases was obtained (GenBank accession number AF024655). Other microsporidian SSU-rRNA sequences, representing all microsporidian taxa for which molecular data are available, were obtained from GenBank (Table 1, legend) as well as an archaeabacterial outgroup (*Halobacterium halobium*, GenBank accession number M11583). If multiple entries for the same microsporidian species existed in the GenBank database, entries from one of our laboratories (NJP) were chosen to minimize the effects of random sequencing errors on alignments and phylogeny. As a consequence, 17 (70%) of the sequences chosen originated from our (NJP) laboratory.

To evaluate the relationship of *A. scoticae* to other microsporidia, its sequence was aligned using the CLUSTAL W program [36]. Two alignments were done; the first was 1472 positions long and the second, also incorporating the SSU-rRNA sequence reported for *Pleistophora anguillarum* that is incomplete at its 3' end, was 1318 positions long. In addition to CLUSTAL W alignments, sequences were aligned manually based on their structural features by using the DCSE editor [28] and structurally aligned microsporidian SSU-rRNA sequences retrieved from the Antwerp database [37]. The aligned sequences were subjected to phylogenetic analysis by using the DNAPARS, NEIGHBOR and DNAML programs from the PHYLIP package [9]. As the microsporidian SSU-rRNA sequences differ substantially in their GC content, additional analysis was performed by using the SEAVIEW and PHYLO_WIN programs [14] that incorporate algorithms compensating for unequal base composition [15]. A second analysis was performed using a newly available program PUZZLE [32, 33] that reconstructs phylogenetic trees from molecular data by the maximum likelihood method, utilizing quartet puzzling tree search and calculation of support for internal branches.

Results

Prevalence and Pathology

The incidence of diseased bees was high. Of 183 examined hosts, both males and females, 90.1 % were visibly infected using light microscopy [24]. There were no outward clinical signs of disease in heavily infected individuals that distinguished them from individuals

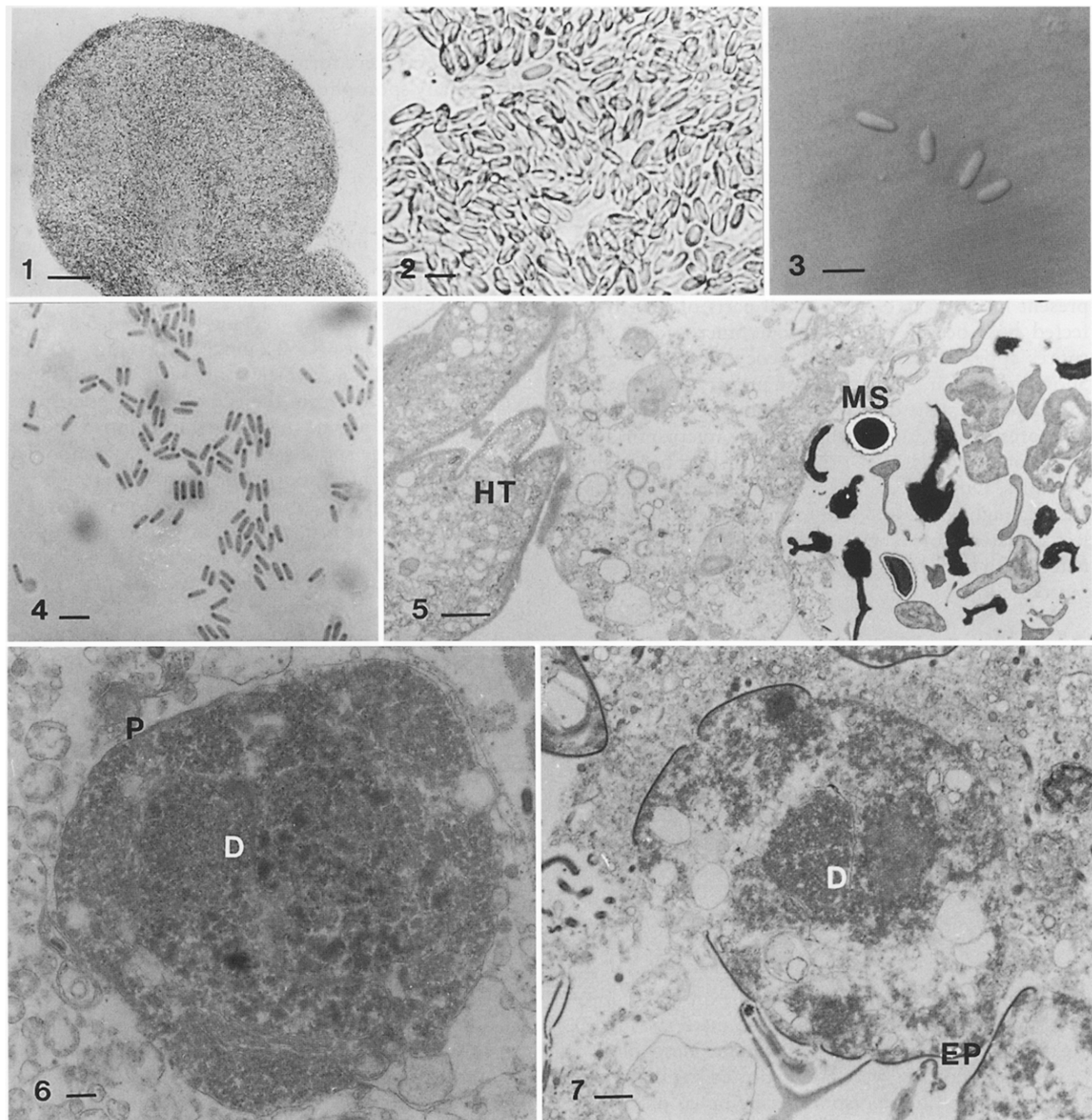


Fig. 1. Adipose tissue developed into an amorphous mass, resembling sacs filled with microsporidian spores. Bar = 50 µm.

Fig. 2. Squash preparation of heavily infected adipose tissue liberating massive numbers of microsporidian spores. Bar = 5 µm.

Fig. 3. Spores prepared in water on a thin agar layer. Interference phase contrast. Bar = 5 µm.

Fig. 4. Spores prepared from adipose tissue stained with Heidenhains iron haematoxylin. Bar = 5 µm.

Fig. 5. Healthy adipose tissue (HT) and infected, disintegrated, adipose tissue with mature spore (MS). Bar = 2 µm.

Fig. 6. Merozoite with plasma membrane (P) and a diplokaryon (D). Bar = 0.25 µm.

Fig. 7. Developing diplokaryotic (D) sporont with the primordium of the exospore (EP) secreted patchily on to the plasma membrane. Bar = 0.5 µm

where the infection was hard to detect. Upon dissection, however, heavily infected bees were easily separated from bees with only light infection based on the appearance of the adipose tissue. The normally pearly-white adipose tissue that covers the terga and sterna of the host bee appeared grey in heavy infected individuals, and seemingly developed into amorphous masses, resembling sacs of microsporidia (Fig. 1). Upon rupturing of such sacs, massive numbers of spores were liberated into the haemocoel without signs of any vesicles or groupings of spores (Fig. 2). Thus, spores were also present in the haemolymph in all parts of heavily infected host bees. Under the light microscope, fresh spores appeared uniform and ovocylindrical (Fig. 3). Spores in fixed and stained squash preparations retained the shape and stained more heavily in one pole (Fig. 4).

Spores or developing stages of the microsporidium were not detected in other tissue of the host bee such as ovarioles, Dufour's gland, ventriculus, small intestine, and Malpighian tubules. As normally seen in field collected material of microsporidia, mature spores dominated, with few observations of the merogonial stage of reproduction.

Presporal stages

Infected adipose tissue became filled with spores and more or less disintegrated. This is illustrated in Fig. 5 where both infected and healthy tissue is represented. Only few vegetative stages could be found and well-fixed complete specimens were unobtainable in this material. Thus the description of the presporal stages is limited. The plasma membrane of vegetative stages was in direct contact with host cytoplasm. They appeared to be diplokaryotic (Fig. 6). Cytoplasmic fission was not observed.

Electron dense material was deposited external to the plasma membrane of merozoites at the onset of sporogony. Apart from this electron dense material (Fig. 7), the diplokaryotic sporonts resembled the merozoites.

Dividing sporonts were not identified but the sporogony is believed to be disporoblastic based on the appearance of sporoblasts and mature spores in infected tissue. The sporogony appeared to be in direct contact with host cytoplasm. The spore wall with plasma membrane, endospore and exospore was seen developing in late sporoblasts and immature spores (Fig. 8).

The mature spore

The spores were formed free in host cell cytoplasm without any sporophorous vesicle.

Mature spores were ovocylindrical, straight to slightly curved. Fresh spores measured $5.6-7.8 \times 2.1-3.5 \mu\text{m}$ (average $6.8 \times 2.7 \mu\text{m}$, $N = 59$) (Fig. 3) whereas spores fixed and stained for TEM measured $4.4-5.8 \times 1.4-2.2 \mu\text{m}$ (average $5.0 \times 1.8 \mu\text{m}$, $N = 12$) (Fig. 9).

The details of emptied spores could only be studied with the electron microscope. Emptied spores, or spores with partly ejected polar filament, were larger than non-germinated spores and measured $5.8-7.1 \times 1.8-2.5 \mu\text{m}$ (average $6.4 \times 2.2 \mu\text{m}$, $N = 11$) (Fig. 10). The approximately 210 nm thick spore wall in both spore types was made up from the exospore, the endospore and the internal plasma membrane. In emptied spores, the surface of the spore wall was somewhat smoother (Fig. 10) than in intact spores; the latter had a rough appearance (Fig. 9). The stratified exospore in both intact and emptied spores had four layers (Fig. 11). An internal single layer (a) was followed by a thicker, more electron dense layer (b). Outside of this electron dense layer, there was another single layer (c) followed by a thin external double layer (d). Internal to the first single layer and external to the double layer, there were additions of indistinct granular material. The exospore measured 24–32 nm in thickness excluding the granular material. The lucent endospore of both intact and emptied spores measured 163–209 nm in thickness.

The polar filament was isofilar and coiled in the posterior and middle part of the spore, and the number of coils varied between 15 and 22. A few coils were sometimes arranged in double layers in the posterior part of the spore. The filament coils had an angle of tilt of the most anterior coil of the polar filament to the long axis of the spore of between 30–5° and the diameter of the filament was 84–89 nm. Four distinct sections could be identified in transversely sectioned filaments: an external unit membrane (d) an external moderately dense ring (c) a thin less electron dense ring (b) a granular centre (a) slightly more electron dense than the second layer (Fig. 12). The filament was attached to the bi-convex anchoring disc at the apical pole of the spore (Fig. 13).

The umbrella-like polar sac that enclosed the anchoring disc stretched down the spore and overlapped approximately 20% of the polaroplast (Fig. 13). The

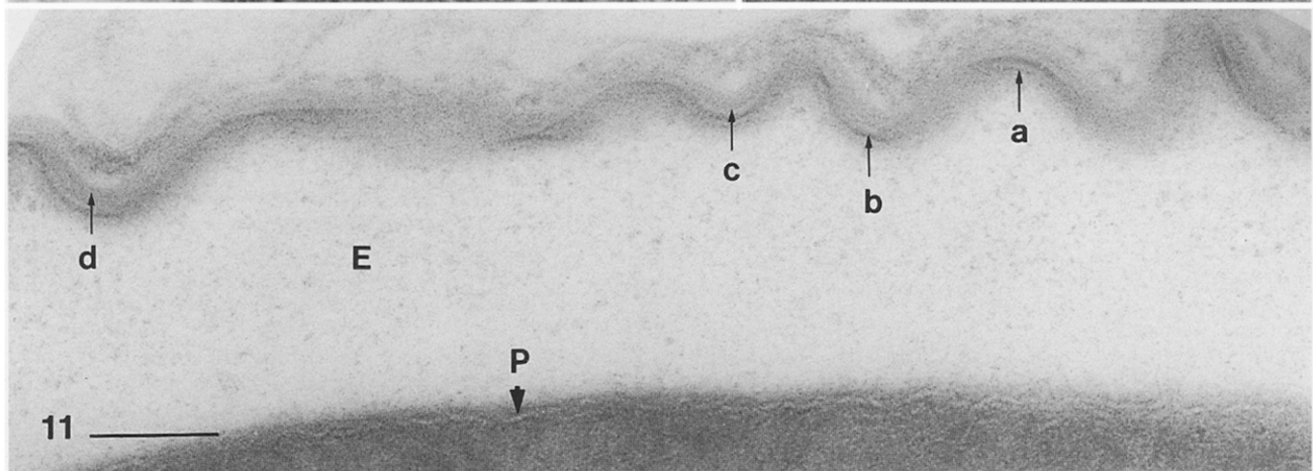
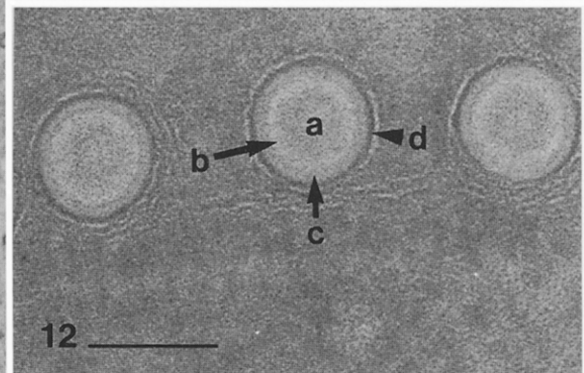
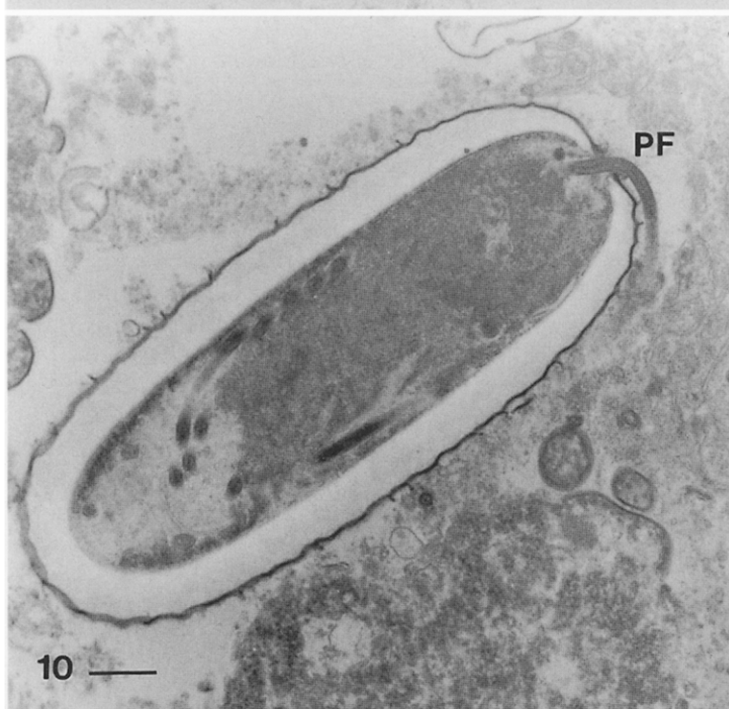
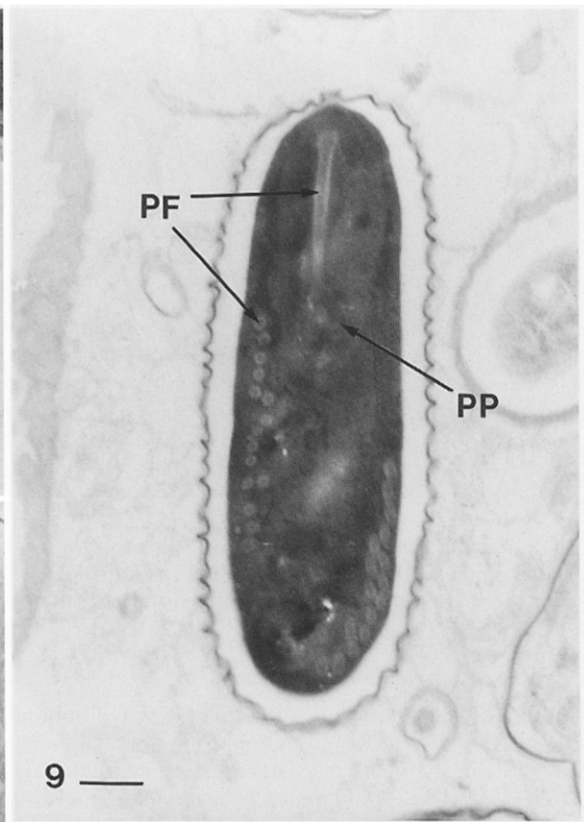
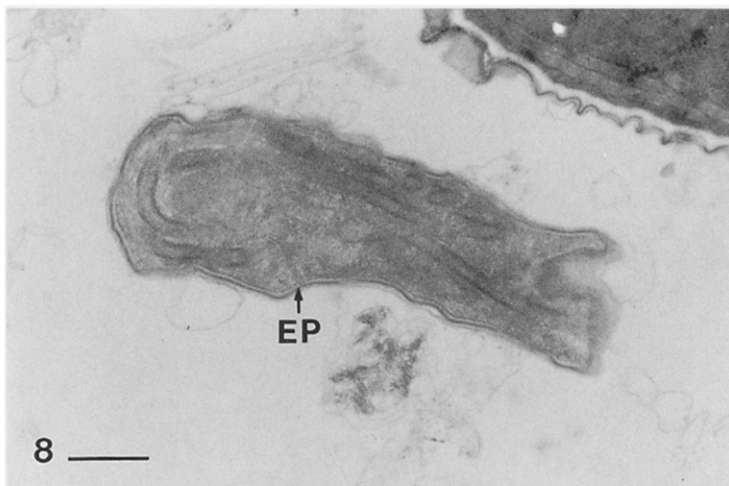
Fig. 8. Late sporoblast/immature spore showing the developing spore wall (EP). Bar = 0.5 μm .

Fig. 9. Longitudinally sectioned mature spore with polar filament (PF) and polaroplast (PP) visible. Bar = 0.5 μm .

Fig. 10. Spore in the process of ejecting the polar filament (PF) inside adipose tissue. Bar = 0.5 μm .

Fig. 11. The spore wall of a mature spore with the plasma membrane (P), the lucent endospore (E) and the four-layered exospore. The layers are indicated a-d in direction outwards. Bar = 0.1 μm .

Fig. 12. Transversally sectioned polar filament coil. The four layers identified are indicated a-d in direction outwards. Bar = 0.1 μm .



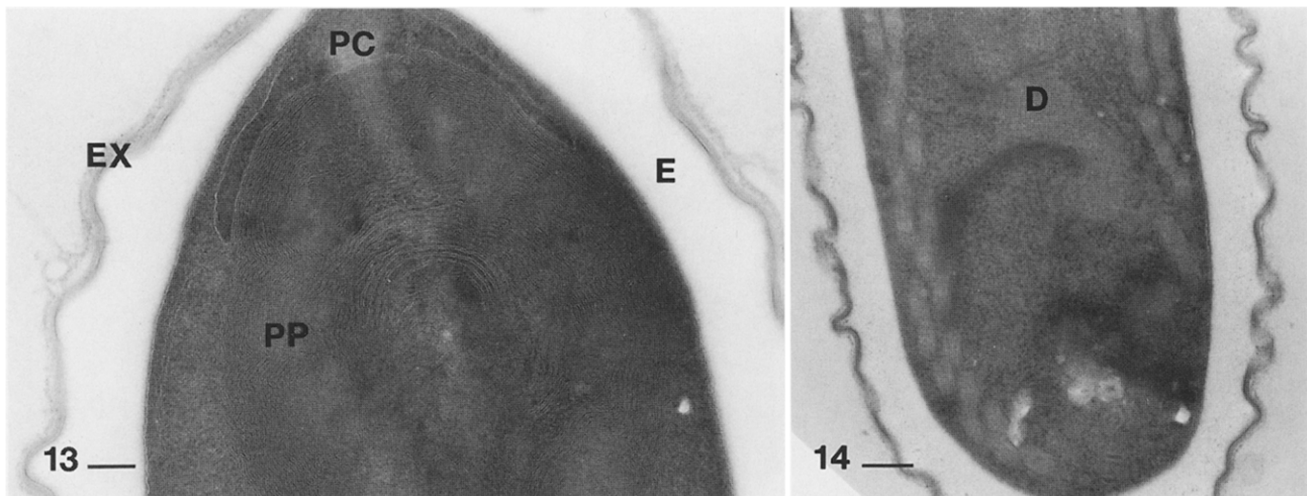


Fig. 13. Apical part of mature spore showing the polar cap (PC), lamellar structure of the anterior polaroplast (PP) and the spore wall with the endospore (E) and exospore (EX). Bar = 0.1 µm.

Fig. 14. Posterior part of mature spore with diplokaryon (D) visible. Bar = 0.2 µm.

Table 1. Base composition (%GC) of the small subunit ribosomal RNA (SSU-rRNA) coding region for all microsporidia available in the GenBank database. The calculation is based on a CLUSTAL W alignment, truncating all sequences to an equal number of alignment columns (1318), including gaps.

Species	%GC
<i>Amblyospora californica</i>	49.0
<i>Amblyospora</i> sp.	48.6
<i>Ameson michaelis</i>	43.4
<i>Antonospora scoticae</i>	62.5
<i>Encephalitozoon (Septata) intestinalis</i>	51.9
<i>Encephalitozoon cuniculi</i>	53.0
<i>Encephalitozoon hellem</i>	48.8
<i>Endoreticulatus schubergi</i>	51.4
<i>Enterocytozoon bieneusi</i>	48.5
<i>Enterocytozoon salmonis</i> *	49.3
<i>Glugea atherinae</i>	51.5
<i>Ichthyosporidium</i> sp.	50.8
<i>Nosema apis</i>	39.1
<i>Nosema bombycis</i>	33.9
<i>Nosema ceranae</i>	36.7
<i>Nosema furnacalis</i>	33.8
<i>Nosema necatrix</i> **	37.1
<i>Nosema oulemae</i>	37.4
<i>Nosema</i> sp.	37.0
<i>Nosema vespula</i>	37.1
<i>Pleistophora anguillarum</i>	54.3
<i>Spraguea lophii</i>	49.4
<i>Vavraia oncoperae</i>	56.8
<i>Vittaforma corneae</i>	48.5

GenBank accession numbers of the SSU-rRNA sequences shown in this table: *Amblyospora californica* – U68473; *Amblyospora* sp. – U68474; *Ameson michaelis* – L15741; *Antonospora scoticae* – AF024655; *Encephalitozoon cuniculi* – L17072; *Encephalitozoon hellem* – L19070; *Endoreticulatus*

anterior polaroplast consisted of closely packed lamellae, approximately 9 nm thick. The posterior polaroplast also consisted of packed lamellae, but these were wider and less uniform than in the anterior polaroplast and extended well beyond the most apical coil of the polar filament (Fig. 9).

In a few cases, a diplokaryon was detected in the electron dense spore, seemingly located in the posterior parts (Fig. 14). No vacuole or clear membrane-bound posterior body was detected in the posterior part of the spore, although the interior of the spore appeared denser in this part in some specimens.

SSU-rRNA coding sequence

The base composition (%GC) of the SSU-rRNA coding sequence for *A. scoticae* was compared to the base composition of all known microsporidian SSU-rRNA sequences. For these calculations, sequences

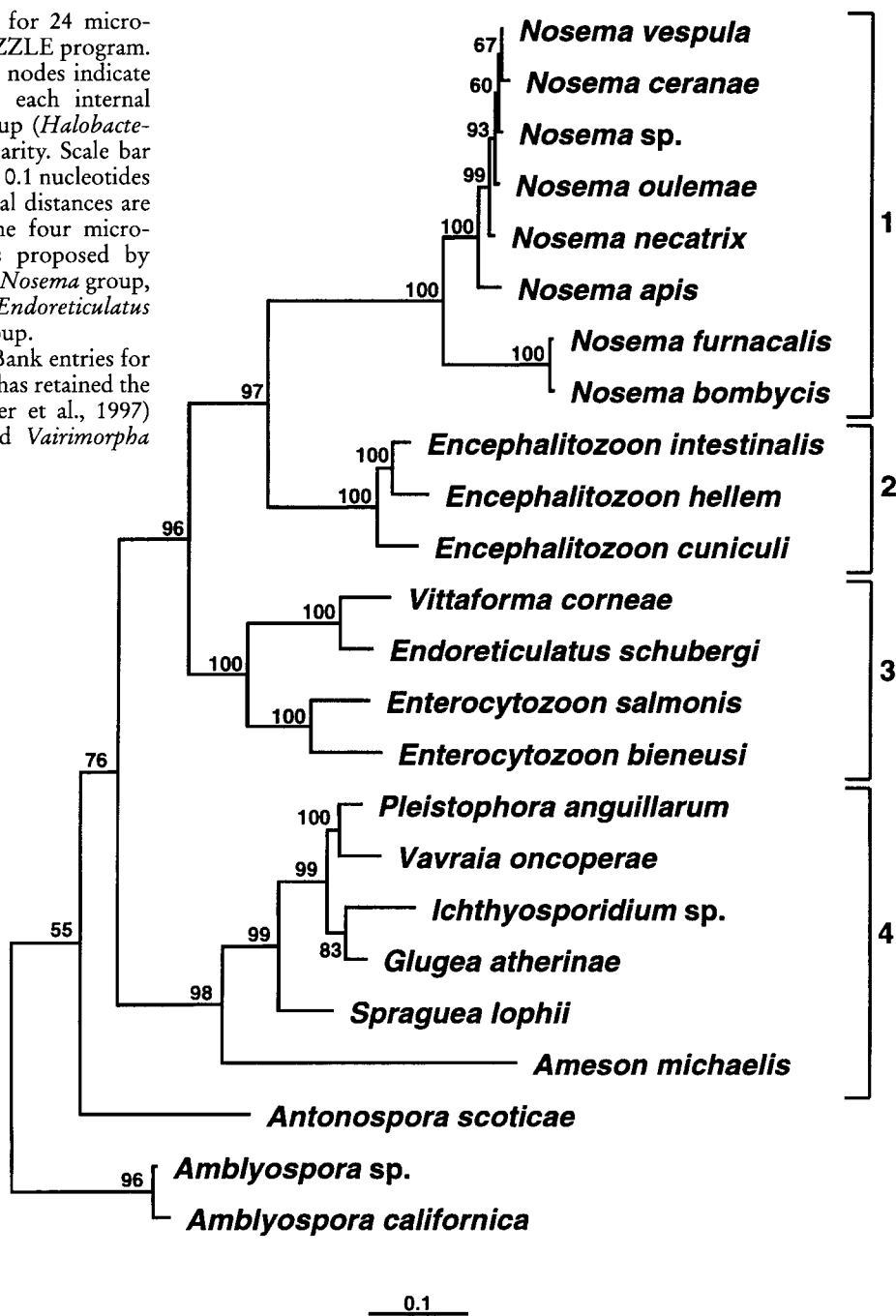
schubergi (*Pleistophora* sp.) – U10342; *Encephalitozoon (Septata) intestinalis* – U09929; *Enterocytozoon bieneusi* – AF024657; *Enterocytozoon salmonis* – U10883*; *Glugea atherinae* – U15987; *Ichthyosporidium* sp. – L39110; *Nosema apis* – U26534; *Nosema bombycis* – U09282; *Nosema ceranae* – U26533; *Nosema furnacalis* – 26532; *Nosema necatrix* – U11051**; *Nosema oulemae* – U27359; *Nosema* sp. – D85501; *Nosema vespula* (*lymantriae*) – U11047; *Pleistophora anguillarum* – U47052; *Spraguea lophii* – AF033197; *Vavraia oncoperae* – X74112; *Vittaforma corneae* – U11046.

* *Enterocytozoon salmonis* has retained the name *Nucleospora salmonis* (Docker et al., 1997)

** *N. necatrix* has been renamed *Vairimorpha necatrix* (Pilley, 1976)

Fig. 15. Maximum likelihood tree for 24 microsporidian taxa generated by the PUZZLE program. Numbers to the left or right of the nodes indicate the quartet puzzling support for each internal branch. The archaeabacterial outgroup (*Halobacterium halobium*) was omitted for clarity. Scale bar indicates an evolutionary distance of 0.1 nucleotides per position in the sequence. Vertical distances are for clarity only. Brackets show the four microsporidian phylogenetic groups, as proposed by Baker et al. (1995). 1 – *Vairimorpha/Nosema* group, 2 – *Encephalitozoon* group, 3 – *Endoreticulatus* group, and 4 – *Ichthyosporidium* group.

Organism names used refer to GenBank entries for coherence with Table 1. *E. salmonis* has retained the name *Nucleospora salmonis* (Docker et al., 1997) and *N. necatrix* has been renamed *Vairimorpha necatrix* (Pilley, 1976).



were first aligned using CLUSTAL W and trimmed at the 5' and 3' regions to equal numbers of alignment columns, including gaps. The length of the alignment, which incorporated the sequence for *Pleistophora anguillarum*, was 1318 columns. As presented in Table 1, the SSU-rRNA sequence of *A. scoticae* has the highest GC content (62.5%) of all microsporidian sequences determined so far, almost twice as high as the SSU-rRNA sequence of *Nosema furnacalis* (33.8%).

Phylogenetic analysis

The observed difference in base composition among microsporidian SSU-rRNA sequences complicates the alignment of these sequences and selection of sites for phylogenetic analysis. Removal of ambiguously aligned regions or using secondary structural features as a basis for alignment resulted in changing only the branch lengths of the phylogenetic tree and not the placement

of the branches. Low bootstrap or quartet puzzling values for certain internal branches remained basically unchanged. Moreover, using algorithms compensating for unequal base distribution did not improve the bootstrap values for these internal branches, nor did it influence the topology of the tree.

Fig. 15 presents the maximum likelihood PUZZLE tree. The division of microsporidia into four main groups (*Vairimorpha/Nosema*, *Encephalitozoon*, *Endoreticulatus*, *Ichthyosporidium*) is identical to that reported earlier by Baker et al. [2]. *Antonospora scoticae*, like the two species of *Amblyospora*, forms a separate early branch. However, the quartet puzzling support for these branches is low (76% and 55%, respectively). Comparable low support was obtained for these branches with bootstrap analysis using the Neighbor Joining method. Parsimony analysis resulted in two most parsimonious trees differing in the placement of the branches in the *Encephalitozoon* group. In both trees, the *Amblyospora* group was placed as a sister taxon to one composed of the *Nosema*, *Encephalitozoon*, and *Endoreticulatus* groups (results not shown).

Discussion

We conclude from the presented material that the microsporidium found in *A. scotica* is a new species. It represents the fourth microsporidium described from the Apoidea and the first in the family Andrenidae.

We found large numbers of empty spores in fixed material (Fig. 10). The presence of empty spores of microsporidia in the host cytoplasm is sometimes interpreted as indicative of intercellular transmission of the parasite [10, 16]. However, in the present case, the possibility that the empty spores represent an artifact caused by handling and fixation cannot be ruled out. Some frozen spores that are thawed also extrude their polar filament under the light microscope in tap water. Although the empty spores are significantly different in size from intact spores, they are believed to be from the same parasite as intact spores based primarily on exospore construction.

All microsporidia found in apid hosts thus far belong to the genus *Nosema* of the family Nosematidae. Within Nosematidae, there are two other genera: *Ichthyosporidium* and *Hirsutosporos* [5]. *Hirsutosporos* contains only one described species, infecting blackflies (Diptera, Simuliidae), in which the exospore of the parasite is formed of homogenous electron-dense material and bears filamentous appendages at the posterior pole [3]. *Ichthyosporidium* contains only two named species, both fish parasites [6]. *Ichthyosporidium giganteum*, producing xenoma with projections interdigitating with host tissue, is the only species in this genus where ultrastructural

data are available [6]. It is also characterized, amongst others, by an exospore that forms a uniform electron-dense layer, but without marked projections [1].

The newly described microsporidium is apansporoblastic, diplokaryotic and develops in direct contact with the host cytoplasm throughout its development. All stages are probably binucleate, and the mature spore form is ovocylindrical. These characteristics would warrant that *A. scoticae* is placed within the family Nosematidae.

Following the key to microsporidian genera by Larsson [18], the new microsporidium described here could be forced into the genus *Nosema* within the Nosematidae. However, members of the heterogeneous genus *Nosema* generally have exospores similar to those of *Ichthyosporidium*, while the described microsporidium from *A. scotica* has an exospore construction, which is markedly different from *Nosema* or other genera in the Nosematidae. The exospore construction of *A. scoticae* is different from, but has resemblance to, the stratified exospore of the basic type of Thelohaniidae [17], and clearly distinguishes *A. scoticae* from members of the genus *Nosema*. Indeed, the exospore primordia and the structure of the mature exospore are important taxonomic characters that have been used to distinguish different groups of the microsporidia [17]. Larsson [17] describes 4 main types of exospore arrangements, further divided into 14 groups. However, the exospore of *A. scoticae* cannot be fitted into any of these groups, with its unusual combination of external double layer and central electron dense layer. This further suggests that this microsporidium does not fit within existing genera.

Furthermore, the molecular data demonstrate that the new microsporidium from *A. scotica* is clearly not related to members of the family Nosematidae. Since classification of microsporidia based on morphological features alone may be inconsistent with the phylogeny based on SSU-rRNA [2, 11], classification to ranks above the genus level for this organism can only be provisional. In addition, insufficient molecular data are available for most species of Nosematidae, as is also the case for most known microsporidia. Thus the higher taxonomic assignment of the new species described here cannot yet be made.

Although a similar spore shape is shared by other genera in Nosematidae, and spore shape sometimes is considered diagnostic for the genus [4], none of the existing genera can accommodate the new species. It may be debated whether the meager information supplied on merogony and sporogony of the parasite warrant the creation of a new genus. However, rather than "increasing the amorphous mass of *Microsporidium* species" [18], we establish the new species and new genus *Antonospora scoticae* for this microsporidium

based on the construction of its exospore and careful analysis of molecular data.

The SSU-rRNA coding region described from *A. scoticae* is longer (1371 bp) than that found from most other microsporidia (1250 bp). Its GC content (62%) is also substantially different from that of known *Nosema* spp. (33.8 to 39.1%). This suggests a large evolutionary distance between members of *Nosema* and the new microsporidium from *A. scoticae*. This large evolutionary distance, not only between it and members of the genus *Nosema* but also between it and any other microsporidium for which molecular data are available, is evident from results of the phylogenetic analysis presented in Fig. 15. The reason for such high divergence in the SSU-rRNA of microsporidia is unclear. This may reflect the natural history of this phylum, or an unusual structure of the microsporidian ribosome.

Debates among proponents of different (morphological vs. molecular) approaches to taxonomy [20, 26] are often as intense and unnecessarily acrimonious as among proponents of different methodologies of molecular systematics [34]. Strong evidence exists that SSU-rRNA-based molecular systematics is useful for the taxonomy of the Protozoa in general [13, 19] and for microsporidia in particular [1, 2, 11, 25]. Since molecular and morphological data do not always concur, there is a need to construct a taxonomic classification in which information on both molecular and morphological characteristics may be integrated. To exclude molecular data in a taxonomic system of microsporidia is ill-advised, just as we need to employ morphological data for species where molecular data are as yet unavailable.

Within molecular systematics, there seems to be no consensus on the choice of alignment methods for molecular sequences or on the choice of phylogenetic methods [34]. Thus it is important to note that observed differences in the topology of the trees obtained by using different alignment and phylogenetic methods were relatively minor in our studies. When the two *Amblyospora* species and *A. scoticae* were excluded, resulting parsimony, neighbor joining (employing different models of substitution) and maximum likelihood trees revealed the same four major microsporidian groups as reported by Baker et al. [2]. Moreover, using raw CLUSTAL W aligned data, manually edited data where poorly aligned regions were excluded, and structurally aligned sequences (see Methods) did not influence the placement of the four major microsporidian groups, changing only the lengths of the branches. Within these groups, the only difference from previously published results [1, 39] was seen within the *Encephalitozoon* group, where our results strongly support the placement of *E. cuniculi* as a sister group to one formed by *E. hellem* and *E. intestinalis*.

Antonospora scoticae forms a separate early branch of the microsporidia and does not form a group with any other microsporidium used in the phylogenetic reconstruction. Nevertheless, the placement of *A. scoticae* and *Amblyospora* branches is not strongly supported by quartet puzzling values. Molecular data from more microsporidian species will be needed to determine the taxonomic position of *A. scoticae*.

Taken alone, morphological evaluation could place *A. scoticae* in the family Nosematidae. However, this is highly inconsistent with the molecular data, and additionally suggests that the Nosematidae is based on characters that are polyphyletic in nature, i.e. formed independently in different groups of microsporidia. Such inconsistencies were observed even in the genus *Nosema*, where upon re-examination of the morphology [30], *Nosema corneum* was renamed *Vittaforma corneae*. This change was independently supported by a SSU-rRNA phylogeny [2]. Thus, our data strongly support the need to re-evaluate the taxonomy of microsporidia. We support the opinion of Baker et al. [2] that phylogenetic trees based on SSU-rRNA sequences may be helpful in the selection of morphological data to reconstruct the systematics of this phylum.

Description

Antonospora n. gen.

Diagnosis. Diplokaryotic merogony. Probably disporoblastic development with all developmental stages in direct contact with host cytoplasm. Spores are ovo-cylindrical and binucleate. The exospore is stratified with four layers. An internal single layer is followed by an electron dense uniform layer, another single layer, followed by an external double layer. Polaroplast of traditional type with an anterior part with closely packed lamellae and a more posterior part with less densely packed lamellae. Polar filament isofilar.

A. scoticae n. sp.

Merogony: As for the genus. No dividing stages observed.

Sporogony: Probably disporoblastic.

Spores: Ovocylindrical. Measurements of spores average $6.8 \times 2.7 \mu\text{m}$ when fresh and $5.0 \times 1.8 \mu\text{m}$ when fixed and stained for TEM. The spore wall is approximately 210 nm thick with the endospore measuring 163–209 nm and with a four-layered exospore. The isofilar polar filament is 84–89 nm wide. It is arranged in 15–22 coils in the posterior part of the spore, with the most posterior part sometimes in two layers. The angle of tilt is approximately 30–35°. A diplokaryon is located in the posterior part of the spore. The polar cap overlies part of the anterior polaroplast, which consists

of closely packed lamellae. An indistinct structure in the posterior part of the spore may represent a postero-some. No posterior vacuole could be seen.

Host tissue involved: adipose tissue in the gaster of the host.

Type host: *Andrena scotica* Perkins, 1916 (Hymenoptera: Andrenidae).

Type locality: Törnbottens Stugby, Öland, SE Sweden, 16° 34' E, 56° 29' N.

Type series: Syntypes on slides No. 970515-1 IF to 970515-8 IF.

Deposition of type: Slides No. 970515-1 IF and 970515-2 IF in the International Protozoan Type slide collection, Smithsonian Institution, Washington DC, USA. Other syntype slides are in the collection of the first author.

Acknowledgements: The authors are grateful for excellent technical assistance using TEM by Hans Ekwall, Marianne Ekwall and Margaretha Hallin. Alexandre J. da Silva was supported by a fellowship from Conselho Nacional de Desenvolvimento Científico e Tecnológico (CNPq) - Programa Rhae, Brazil. The authors thank Drs. Govinda S. Visvesvara and Ronny Larsson for helpful suggestions on the manuscript.

References

- Baker M. D., Vossbrinck C. R., Maddox J. V. and Undeen A. H. (1994): Phylogenetic relationships among *Vairimorpha* and *Nosema* species (Microspora) based on ribosomal RNA sequence data. *J. Invertebr. Pathol.* 64, 100–106.
- Baker M. D., Vossbrinck C. R., Didier E. S., Maddox J. V. and Shadduck J. A. (1995): Small subunit ribosomal DNA phylogeny of various microsporidia with emphasis on AIDS related forms. *J. Euk. Microbiol.* 42, 564–570.
- Batson B. S. (1983): A light and electron microscopical study of *Hirsutosporos austrosimulii* gen. n., sp. n., (Microspora: Nosematidae), a parasite of *Austrosimulium* sp. (Diptera: Simuliidae) in New Zealand. *Protistologica* 19, 263–280.
- Bylén E. K. C. and Larsson R. (1994): Ultrastructural study and description of *Pernicivesicula gracilis* gen. et sp. nov. (Microspora, Pereziidae) a rod-shaped microsporidium of midge larvae, *Pentaneurella* sp. (Diptera, Chironomidae), in Sweden. *Europ. J. Protistol.* 30, 139–150.
- Canning E. U. (1990): Phylum Microspora. In: Margulis, L., Corliss, J. O., Melkonian, M., Chapman, D. and Jones J. (eds): *Handbook of Protocista*, pp. 53–72. Bartlett, Boston, Boston.
- Casal G. and Azevedo C. (1995): New ultrastructural data on the microsporidian *Ichthyosporidium giganteum* infecting the marine teleostean fish *Ctenolabrus rupestris* (L.). *J. Fish Dis.* 18, 191–194.
- Docker M. F., Kent M. L., Hervio D. M. L., Khattri J. S., Weiss L. M., Cali, A. and Devlin, R. H. (1997): Ribosomal DNA sequence of *Nucleospora salmonis* Hedrick, Groff and Baxa, 1991 (Microsporea: Enterocytozoonidae): Implications for phylogeny and nomenclature. *J. Euk. Microbiol.* 44, 55–60.
- Fantham H. B. and Porter A. (1914): The morphology, biology and economic importance of *Nosema bombi*, n. sp., parasitic in various humble bees (*Bombus spp.*). *Ann. Trop. Med. Parasitol.* 8, 623–638.
- Felsenstein J. (1989): PHYLIP – Phylogeny inference package. *Cladistics*, 5, 164166.
- Fries I. (1989): Observations on the development and transmission of *Nosema apis* Z. in the ventriculus of the honey bee. *J. Apic. Res.* 28, 107–117.
- Fries I., Feng F., da Silva A., Slemenda S. B. and Pieniazek N. J. (1996): *Nosema ceranae* n. sp. (Microspora, Nosematidae), morphological and molecular characterization of a microsporidian parasite of the Asian honey bee *Apis cerana* (Hymenoptera, Apidae). *Europ. J. Protistol.* 32, 356–365.
- Fries I., Granados R. R. and Morse R. A. (1992): Intracellular germination of spores of *Nosema apis* Z. *Apidologie* 23, 61–71.
- Gajadhar A. A., Marquardt W. C., Hall R., Gunderson J., Ariztia-Carmona E. V. and Sogin M. L. (1991): Ribosomal RNA sequences of *Sarcocystis muris*, *Theileria annulata* and *Cryptosporidium cohnii* reveal evolutionary relationships among apicomplexans, dinoflagellates, and ciliates. *Mol. Biochem. Parasitol.* 45, 147–154.
- Galtier N., Gouy M. and Gautier C. (1996): SEAVIEW and PHYLO_WIN: two graphic tools for sequence alignment and molecular phylogeny. *Comput. Appl. Biosci.* 12, 543–548.
- Galtier N. and Gouy M. (1995): Inferring phylogenies from DNA sequences of unequal base compositions. *Proc. Natl. Acad. Sci. USA* 92, 11317–11321.
- Kurtti J. T., Tsang R. K. and Brooks M. A. (1983): The spread of infection by the microsporidian *Nosema distriae*, in insect cell lines. *J. Protozool.* 30, 652–657.
- Larsson R. (1986): Ultrastructure, function, and classification of Microsporidia. *Progr. Protistol.* 1, 325–390.
- Larsson R. (1988): Identification of microsporidian genera (Protozoa, Microspora) – a guide with comments on taxonomy. *Arch. Protistenkd.* 136, 1–37.
- Leipe D. D., Tong S. M., Goggin C. L., Slemenda S. B., Pieniazek N. J. and Sogin M. L. (1996): 16S-like rDNA sequences from *Developayella elegans*, *Labrynthus haliotidis*, and *Proteromonas lacertae* confirm that the stramenopiles are a primarily heterotrophic group. *Europ. J. Protistol.* 32, 449–458.
- Marquardt W. C. (1997): The taxonomy of Cyclospora – letters to the editor. *Emerg. Infect. Dis.* 3, 579–580.
- McIvor C. A. and Malone L. A. (1995): *Nosema bombi*, a microsporidian pathogen of the bumble bee *Bombus terrestris* (L.). *New Zealand J. Zool.* 22, 25–31.
- Michener C. D. (1974): The social behavior of the Bees. Belknap Press, Cambridge.
- Paxton R. J., Fries I., Pieniazek N. J. and Tengö J. (1997): High incidence of infection of an undescribed microsporidium (Microspora) in the communal bee *Andrena scotica* (Hymenoptera, Andrenidae). *Apidologie* 28, 129–141.
- Pieniazek N. J., da Silva A., Slemenda S. B., Visvesvara G. S., Kurtti T. J. and Yasunaga C. (1996): *Nosema trichoplusiae* is a synonym of *Nosema bombycis* based on the sequence of the small subunit ribosomal RNA coding region. *J. Invertebr. Pathol.* 67, 316–317.

- 26 Pieniazek N. J. and Herwaldt B. L. (1997): The taxonomy of Cyclospora – reply to W.C. Marquardt. *Emerg. Infect. Dis.* 3, 580.
- 27 Pilley B. M. (1976): A new genus, *Vairimorpha* (Protozoa: Microsporida), for *Nosema necatrix* Kramer 1965: Pathogenicity and life cycle in *Spodoptera exempta* (Lepidoptera: Noctuidae). *J. Invertebr. Pathol.* 28, 177–183.
- 28 de Rijk P. and de Wachter R. (1993) DCSE, an interactive tool for sequence alignment and secondary structure research. *Comput. Appl. Biosci.* 9, 735–740.
- 29 da Silva A. J., Bornay-Llinares F. J., del Aguila de la Puente C., Moura H., Peralta J. M., Sobottka I., Schwartz D. A., Visvesvara G. S., Slemenda S. B. and Pieniazek N. J. (1997): Diagnosis of *Enterocytozoon bieneusi* (Microsporidia) infections by polymerase chain reaction in stool samples using primers based on the region coding for small-subunit ribosomal RNA. *Arch. Pathol. Lab. Med.* 121, 874–879.
- 30 Silveira, H. and Canning E. U. (1995): *Vittaforma cornea* n. comb. for the human microsporidium *Nosema corneum* Shadduck, Meccoli, Davis & Font, 1990, based on its ultrastructure in the liver of experimentally infected athymic mice. *J. Euk. Microbiol.* 42, 158–165.
- 31 Sprague V., Becnel J. J. and Hazard E. I. (1992): Taxonomy of phylum Microspora. *Crit. Rev. Microbiol.* 18, 285–395.
- 32 Strimmer K. and von Haeseler A. (1996): Quartet puzzling: a quartet maximum likelihood method for reconstructing tree topologies. *Mol. Biol. Evol.* 13, 964–969.
- 33 Strimmer K. and von Haeseler A. (1997): Likelihood-mapping: a simple method to visualize phylogenetic content of a sequence alignment. *Proc. Natl. Acad. Sci. (USA)* 94, 6815–6819.
- 34 Swofford D., Olsen G. J., Waddell P. J. and Hillis D. M. (1996): Phylogenetic Interference. In: Hillis D. M., Moritz C., Marble B. (eds.): *Molecular Systematics*, pp. 407–514. Sinauer Associates, Inc., Sunderland, Massachusetts.
- 35 Tindall K. R. and Kunkel T. A. (1988): Fidelity of DNA synthesis by the *Thermus aquaticus* DNA polymerase. *Biochemistry* 27, 6008–6013.
- 36 Thompson J. D., Higgins D. G. and Gibson T. J. (1994): CLUSTAL W: improving the sensitivity of progressive multiple sequence alignment through sequence weighting, position specific gap penalties and weight matrix choice. *Nucleic Acids Res.* 22, 4673–4680.
- 37 Van der Peer Y., Jansen J., De Rijk P. and De Wachter R. (1997): Database on the structure of small ribosomal sub-unit RNA. *Nucleic Acids Res.* 24, 111–116.
- 38 Zander E. (1909): Tierische Parasiten als Krankheitserreger bei der Biene. *Leipz. Bienenztg.* 24, 147–150, 164–166.
- 39 Zhu X., Wittner M., Tanowitz H. B., Cali A. and Weiss L. M. (1994): Ribosomal RNA sequences of *Enterocytozoon bieneusi*, *Septata intestinalis*, and *Amesom michaelis*: Phylogenetic construction and structural correspondence. *J. Euk. Microbiol.* 41, 204–209.